GIS for seismic risk evaluation of piled foundations in land subsidence area

Évaluation des hazards induit par séismic pour les foundations sur pieux dans lés regions de tassement du terrain utilisant une système d'information geographique

K.Yasuhara & S.Murakami – *Department of Urban & Civil Engineering, Ibaraki University, Hitachi, Ibaraki, Japan*

ABSTRACT: The results from the analysis of risk for pile foundations undergoing seismic subsidence in the Northern Kanto plain in Japan is visualised using GIS. The analytical procedure is based upon Chang's method for evaluating the bending moment of piles in land subsidence areas combined with the results from settlement prediction and seismic analysis and a consideration of the effects of active faults existing in the objective area. The results from the seismic risk evaluation of piled foundations undergoing land subsidence are visualized as a GIS hazard map which may be utilized for taking countermeasures against earthquake-induced disasters.

RÉSUMÉ: L'analyse du risque du tassement sismique pour les fondations sur pieux en Kanto en Japon est visualisé utilisant GIS. L'analyse du Chang pour calculer le flechissement des pieux dans les zones de tassement est utilisé avec les résultats du prediction du tassement et l'analyse sismique considerant l'efffét du failles actifs dans la zone sous consideration. Les résultats sont visualises avec une carte d'hasard du type GIS qui peut etre utilise pour prendre les actions contre les calamités séisme.

1 INTRODUCTION

Nearly 80% of land subsidence due to groundwater abstraction in Japan takes place in the Northern Kanto Plain whose area covers the five prefectures as illustrated in Fig. 1, namely, Saitama, Gunma, Tochigi, Ibaraki and Chiba. According to recent subsidence records, the average amount of subsidence in this area due to groundwater abstraction for agricultural, industrial, and drinking purposes has been approximately 5cm every year although the situation is different depending on the prefecture.

Land subsidence in an area with nearby active faults may also increase the possibility of severe damage due to large earthquakes such as the Great Hanshin Earthquake (1995). Therefore, the infrastructure and buildings in land subsidence areas with the possibility of large earthquakes are exposed to further risk. The Northern Kanto plain or the Niigata plain in Japan can be counted as examples of this situation. In this respect, it is important to evaluate a seismic risk triggered by great settlements in a whole land subsidence area.

The first part of the paper describes seismic risk analysis of piled foundations under land subsidence. A simplified method for predicting future settlements using observed one and a modified method for forecasting ground surface accelerations considering existing active faults are described. The latter part of this study describes the analysis of seismic risk for piled foundations in the Northern Kanto plain which has been the area in Japan most severely damaged by land subsidence.

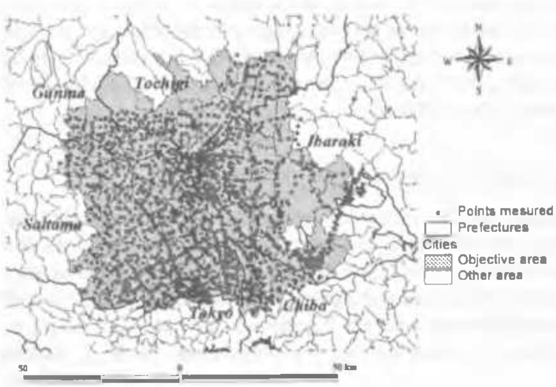

Figure 1. Objective area and locations for measuring settlements.

For purpose of this study, a large quantity of geographical information including the regional characteristics is needed. An attempt was made to estimate the total risk using a Geographical Information System (GIS). GIS is a system capable of investigating, analysing and representing the geographical information related to spatial measurement and phase of natural environments and human activities. GIS is characterized by being capable of treating comprehensively different styles of data and then visualising the analytical results. The information necessary for seismic risk analyses using the method that will be described later is the distribution of ground surface accelerations due to earthquakes and accumulated settlements due to land subsidence. Both sets of information are obtained from numerical data available at the National Land Agency and documentary data available from the five local governments.

2 SEISMIC RISK ANALYSIS OF PILES FOUNDATIONS UNDER LAND SUBSIDENCE

Land subsidence induces not only direct damage such as uneven settlements of structures but also potential damage to infrastructures caused by such events as a flooding in a river or high tides at the shoreline. Piled foundations in land subsidence areas, for example, become unstable due to:

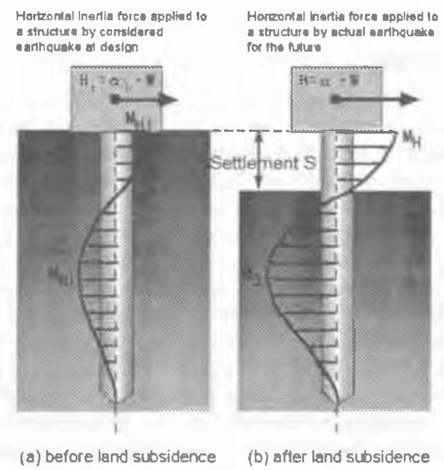

Figure 2. Pile during earthquake before and after land subsidence.

i) negative friction causing downdrag

ii) increased bending moments from the top downwards

An attempt has been made to define an index for the earthquake-induced risk for bearing piled foundations by considering the item (ii) above only. Fig. 2 schematically illustrates the bending moment distribution during earthquakes with acceleration α. The pile head rotation is constrained by the structure. It is postulated that the pile becomes unstable or fails due to an increase in rotational or horizontal movement induced by inertial forces. This study does not consider the lateral movement and liquefaction of ground triggered by earthquakes. In order to define a seismic risk index for piled foundations, it is assumed that the seismic risk can be expressed in terms of the increase in bending moment ratio multiplied by the increase in acceleration ratio in comparison with that before the earthquakes.

According to the linear elastic ground reaction method proposed by Chang (1937), the variation of bending moment of the pile, M_G, with depth when undergoing subsidence, S, due to abstraction of groundwater is given by:

$$M_G = -H\frac{\sqrt{1+(\beta S)^2}}{2\beta}\exp[-\tan^{-1}(\frac{1}{\beta S})] \quad (1)$$

where

$$\beta = \sqrt[4]{\frac{k_h B}{4EI}} \quad (2)$$

$$H = \alpha W \quad (3)$$

where k_h = the coefficient of horizontal ground reaction; B = the diameter of the pile; EI = the bending stiffness of the pile; H = horizontal force; α = earthquake-induced acceleration; and W = the weight of the overlying structure. In the case of S = 0, we have the following relations for M_{Gi} and H_i, respectively, corresponding to the initial condition:

$$M_{Gi} = -\frac{H_i}{2\beta}\exp(-\frac{\pi}{2}) \quad (4)$$

$$H_i = \alpha_i W \quad (5)$$

where α_i = the design acceleration postulated before subsidence. By combining Eq. (1) with (4) and introducing the risk parameter (the inverse value of the safety factor) of the pile for bending moment, the overall risk parameter n of the pile, D, due to land subsidence can be defined as:

$$D = \frac{M_G}{M_C} = \frac{1}{n}R_\alpha R_G \quad (6)$$

where M_c = the allowable bending moment of the pile; $R = \alpha/\alpha_i$, and R_G is given by:

$$R_G = \sqrt{(1+\beta\cdot S)^2}\exp\{\tan^{-1}(\beta\cdot S)\} \quad (7)$$

3 OBSERVATIONAL PREDICTION OF LAND SUBSIDENCE AND ITS APPLICATION

3.1 *A Simplified Procedure*

The amount of land subsidence and its variation with time are normally evaluated by adopting one-dimensional consolidation theory which is modified to take into account the variation in live loads due to seasonal changes in groundwater level. To achieve this and in particular, to prevent disasters to the infrastructure and to regulate groundwater abstraction, we need a great deal of information on geotechnical properties from field and laboratory investigations over the whole area under consideration. However, this is not always feasible from the viewpoint of expense and time. To overcome this difficulty, a simplified method is proposed which is capable of forecasting the future time-settlement relations based upon the information presently available regarding settlements due to groundwater pumping. Strictly speaking, the solution of one-dimensional consolidation theory cannot be directly applied to land subsidence due to groundwater abstraction. However, it is used here as a first approximation, such that settlements due to groundwater pumping can be simply expressed as follows:

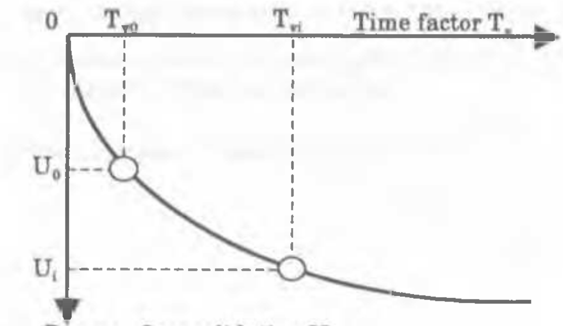

Figure 3. U versus T_v relation.

$$S = S_f \cdot U \quad (8a)$$

$$U = 1 - \frac{4}{\pi^2}\sum_{n=0}^{\infty}\frac{1}{a_n^2}\exp(-a_n^2 T_v) \quad (8b)$$

where S_f = final settlement; U = degree of consolidation; and T_v = time factor. When we consider the interval between two time factors of T_{v0} and T_{vi}, as shown in Fig. 3, the difference, δU_i, in degree of consolidation yields:

$$\delta U_i = U_i - U_0 = \sum_{n=0}^{\infty}\{\frac{2}{a_n^2}\exp(-a_n^2 T_{v0}) - \frac{2}{a_n^2}\exp(-a_n^2 T_{vi})\} \quad (9)$$

In the above equation, by replacing $T_{vi} - T_{v0}$ as δT_v and then neglecting the difference in inherent values after the second order in the consolidation theory solution , Eq. (9) leads to:

$$\delta U_i = \frac{8}{\pi^2}\exp(-\frac{T_{v0}}{4})\{1-\exp(-\frac{\delta T_{vi}}{4})\} \quad (10)$$

By referring to Fig. 2(b), Eq. (4) can be rewritten as:

$$\delta S_i = S_{p0}\{1-\exp(-C_R\delta t_i)\} \quad (11)$$

where S_{po} = the residual settlement expected from the present time until the termination of subsidence under the assumption that the groundwater variation is kept the same as observed at the present time; and C_R = parameter corresponding to settlement strain rate. These are given by:

$$S_{po} = S_{rf} = \frac{8}{\pi^2}\exp(-\frac{T_{v0}}{4}) \quad (12a)$$

$$C_R = \frac{T_{vi}}{t_i} = \frac{4c_v}{H_d^2} \quad (12b)$$

where $S_{r,f}$ = total residual settlement; T_{vo}, T_{vi} are time factors at the start of settlement measurements and an arbitrary time during subsidence respectively; t_i = another arbitrary time during subsidence; c_v = coefficient of consolidation; and H_d = the maximum length of drainage path for the clay layer. If instead of such soil parameters as c_v, H_d and T_v two parameters, S_{po} and C_R, denoted by Eqs. (12a) and (12b) can be determined by using a statistical analysis of previously observed settlement records, the amount of settlement and settlement versus elapsed time relations can be obtained using the "non-linear least squares method" (Murakami et. al.; 1998,2000a,2000b) .

3.2 *Application to Field Measurements*

Applicability of the method proposed above is illustrated by comparing the calculated settlements with those observed. The two parameters $S_{p,o}$ and C_R were determined by a statistical analysis of land subsidence settlement-time records from 1970 until 1990 at 1,282 locations in the Northern Kanto plain in Japan, as shown in Fig. 1, covering the five prefectures: Tochigi, Gunma,

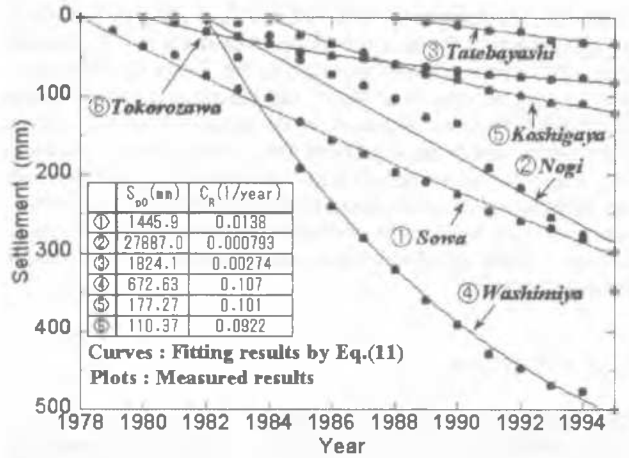

Figure 4. Comparison between observed and calculated settlements versus time relation.

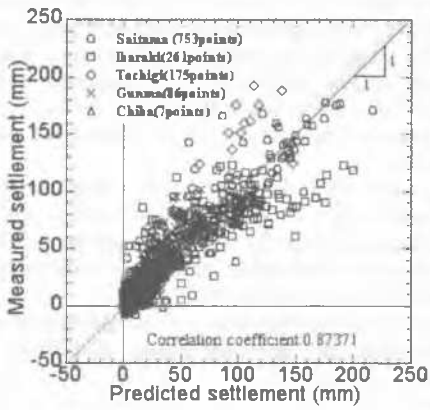

Figure 5. Comparison for observed and calculated settlements.

Saitama, Chiba and Ibaraki. Typical variations of settlements and groundwater level with time for several locations are shown in Fig. 4. It was found that the variation of groundwater level and amount of settlements with elapsed time is location dependent. One of the characteristic features of Fig. 4 is that observed fluctuations in settlements followed seasonal changes in groundwater level.

The above-mentioned procedure was applied to the previously observed settlement versus time records accumulated in the Northern Kanto district for approximately the last twenty years. Typical examples of observed and calculated settlement versus time relations for records from 1975 to 1995 are shown in Fig. 5. The relations for total observed and predicted settlements are given in Fig. 5. The comparisons in Fig. 4 and Fig. 5 are in fairly good agreement with each other.

3.3 *Future Settlement Prediction and its Representation using GIS*

Following the above-mentioned procedure for predicting land subsidence settlements using the previously observed field records at a total of 1,282 locations, the future prediction of settlements was conducted for the 5 years from 1998 to 2002. The results are represented and illustrated in Fig. 6 as a land subsidence hazard map in the Northern Kanto plain using GIS. It is predicted that severe settlements will probably accumulate in some areas if the groundwater is abstracted with continuous variations in groundwater level, although there is a tendency for gradually decreasing settlements in most areas in the Northern Kanto plain. Considering the possibility that large earthquakes can occur in this area, it is suggested that through further investigation the potential for disastrous land subsidence from anticipated earthquakes could be demonstrated using a hazard map developed using GIS.

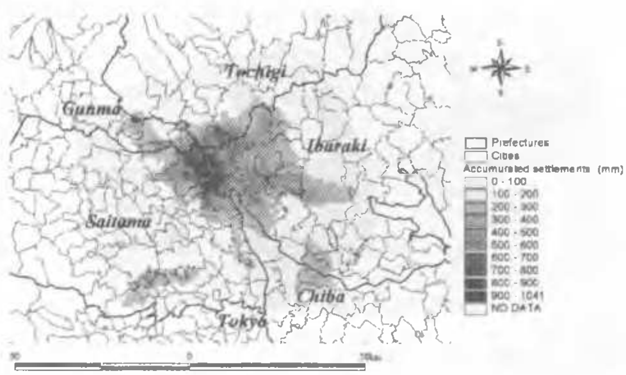

Figure 6. Land subsidence map.

4 EVALUATION OF MAXIMUM ACCELERATION THROUGH SEISMIC RISK ANALYSIS

4.1 *Procedure for Risk Analysis*

To determine the distribution of acceleration induced by earthquakes in the Northern Kanto area, a seismic risk analysis based on a probabilistic model has been carried out. The analysis is based on both data for the geomorphologic discrete and the active faults in this area A computer program modified from EQRISK by McGuire (1976) was adopted.

When the probability of occurrence of earthquakes with an excess acceleration α in the coming t years is given by v_i, the probability of occurrence, v_o, of earthquakes with acceleration exceeding α yields:

$$v_o(\alpha) = \sum_{i=1}^{n} v_i q_i(\alpha) \tag{13}$$

where q_i (α) is the percentage exceeding a certain strength of earthquake motion, y. The acceleration corresponding to a certain value of occurrence rate can be predicted when the occurrence rate, v_o, corresponding to a certain acceleration, α, is given. Thus, the maximum acceleration due to earthquakes can be predicted using this procedure.

To conduct the calculation following the above procedure, the values of α_i and q_i at an earthquake area, need to be determined. To do this, the following two models are used according to whether the objective area would be influenced by active faults or not.

(i) For an area in the vicinity of active faults : a characteristic model was used. This model is based on the assumption that a major earthquake due to an active fault occurs only when the fault is completely destroyed. In addition, we adopt the relation for distance attenuation proposed by Fukushima and Tanaka (1990) as:

$$\log\alpha = aM_s - \log(R + d10^{aM_s}) - bR + c \tag{14}$$

where α = acceleration; M_s = magnitude of surface wave; R = distance from epicenter; a, b, c and d are constants equal to 0.041, 0.0034, 1.30, and 0.032. M_s included in Eq. (14) is equal to:

$$M_s \equiv M_j = \frac{\log L + 2.9}{0.6} \tag{15}$$

where M_j = the magnitude defined by the Meteorological Agency; and L = the distance of fault. Besides, the occurrence rate, v, is:

$$v(\alpha) = \frac{s}{10^{1.9} L} \tag{16}$$

where s = the average displacement rate of the fault (mm/year).
(ii) For earthquakes other than those with the magnitude stated in (i) above : the b-value model proposed by Inoue and Kanda (1993) which is based on the postulate that the frequency of occurrence of earthquakes becomes less with increasing magnitude was used.

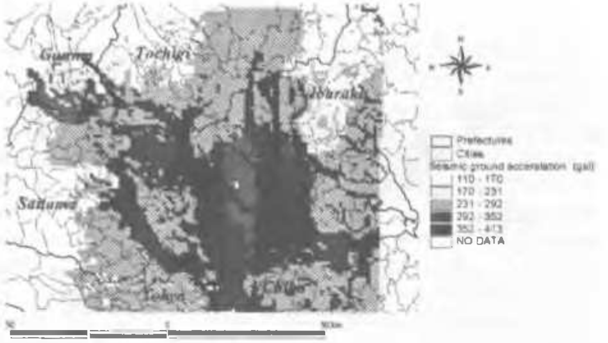

Figure 7 Seismic ground accelaration map.

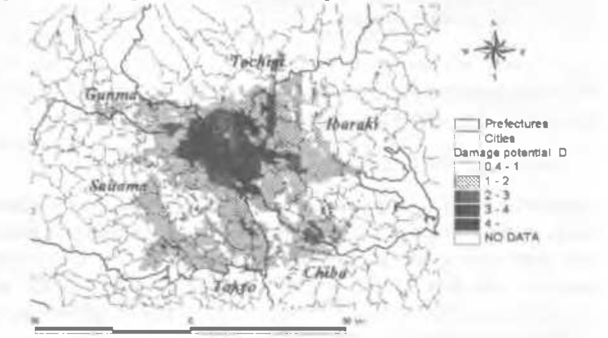

Figure 8 Distribution of seismic risk for piled foundations.

4.2 *Results of Analysis*

The faults used for calculation of earthquake-induced accelerations were those that are included in the widely ranging data collated by the National Land Agency of Japan and whose locations, average displacement rate and length are already known. The parameter proposed by Inoue and Kanda (1993) was used for the area without being influenced by the active faults. Using these parameters, the seismic risk analysis was performed for earthquakes with a return period with 50 years. A further correction was made to the acceleration estimated using the above methods. The correction coefficient corresponding to the National Land Agency geomorphologic classification of each location is 0.6 for mountainous and hilly sites (I grade), 1.39 for lowland, natural dykes and sandbanks (II grade), and 1.0 for other sites (III grade), respectively. The objective area covers the five prefectures in the Northern Kanto plain illustrated in Fig. 1 divided into 1km squares The area was 114km west to east and 102km north to south. The distribution of acceleration calculated using the procedures above is demonstrated in Fig. 7. It is indicated from this figure that:

1) there are some areas belonging to the third grade in Saitama which are in excess of 350 to 400 gal acceleration.
2) the acceleration exceeds 200 gal in most of the objective region.

Therefore, in these areas additional attention should be paid to seismic-triggered instability of piled foundations in cases of severe land subsidence.

5 GIS VISUALIZATION FOR SEISMIC RISK OF PILED FOUNDATIONS IN LAND SUBSIDENCE AREAS

A seismic risk analysis for piled foundations in land subsidence areas was carried out using Eq. (6) combining the results from both settlement analysis and seismic risk analysis in the Northern Kanto plain objective area. The results were visualized using GIS. The parameters α_i and S necessary for analyses were determined as follows:

i) α_i was the acceleration calculated by the seismic risk analysis for earthquakes with a 50 year return period.

ii) S was the settlement accumulated for the period from 1981 to 2010, using the procedure as described previously.

It was also assumed in the analyses that α_i is 198 gal, β was 0.2 for soft ground in the land subsidence area and n is 2.0 was used in Eq. (6). The results are presented in Fig. 8 as a GIS visualization. It can be seen from Fig. 8 that the seismic risk for piled foundations becomes increased in the areas in Ibaraki, Tochigi and Saitama which have suffered from severe land subsidence. This suggests that we should take countermeasures to cope with this situation of potential seismic-induced damage in land subsidence areas in addition to obvious damage such as inclination, uneven settlements of structures, and possible failure of under ground structures.

6 CONCLUSIONS

The results can be summarized as follows :

1) A simplified method for predicting future trends using observed settlements has been proposed and the applicability of the model has been verified by comparing the predicted and measured results at 1,282 points over the area. Using GIS, future land subsidence has been visualized on a hazard map.
2) A method proposed for estimating the seismic risk for piled foundations in land subsidence area requires information on the distribution of accelerations triggered by earthquakes and the magnitude of present and future settlements due to land subsidence.
3) It is suggested from the analysis that due to active faults an average acceleration of 200 gal takes place in the objective area. The seismic risk for piled foundations additionally increases in the land subsidence area. This is more easily understood from the GIS visualization.
4) From the viewpoint of seismic risk analysis countermeasures should be taken for land subsidence, in addition to those against direct damage.

ACKNOWLEDGEMENTS

The authors would like to express their sincere thanks to Prof. R.Inoue (Ibaraki University, Japan) for cooperation in performing the seismic risk analysis. The authors wish to express their sincere thanks to Miss Fukuda (Fukizawa Kensetsu Consultant Corporation, Japan) for helping us to make the database.

REFERENCES

Chang, Y.L. 1937. Discussion on "Lateral pile-loading test", by Feagin, Trans., ASCE, pp. 272 - 278.

Fukushima,Y..and Tanaka,T. 1990. A new attenuation relation for peak acceleration of strong earthquake motion in Japan, *Bulletin of the Seismological Society of America*, No. 80, pp. 757 - 783.

Inoue,C..and Kanda,J. 1993. Earthquake risk analysis with consideration of seismic area in the plate boundary earthquake, *Proc. Japan Society of Architecture (Structural Division)*, 443, 35-43, (in Japanese).

McGuire, R. K. 1976. Evaluation of the sites for earthquake risk (EQRISK), *A computer program distributed by NISEE/Computer applications.*

Murakami, S., Yasuhara, K. & Murata, F. 1998. Land subsidence prediction using a Geographical Information System (GIS), *Proc. Intern'l Symp. Lowland Technology*, Vol 1, pp.507–512, Saga, Japan.

Murakami, S., Yasuhara, K. & Murata, F. 2000a. Land subsidence and its visualization using Geological Information System (GIS), *Proc. Intn'l Symp. Groundwater 2000*, pp.79-84 , Urawa, Saitama, Japan.

Murakami. S., Yasuhara, K., & Murata, F. 2000b. GIS for land subsidence evaluation in Northern Kanto Plain, *Proc. 6th Intn'l Symp. Land Subsidence*, Vol. 2, p.219-228.